Progress In Electromagnetics Research M, Vol. 41, 105–114, 2015

Effect of Temperature on Nanocomposite of Metal Nanoparticles in Photonic Crystals

Nambi R. Ramanujam[1], Kuladaisamy S. Joseph Wilson[2, *], and Vasan Revathy[2]

Abstract—We theoretically investigate the photonic band gaps in one-dimensional photonic crystals based on nanocomposite of silver nanoparticles. The dielectric permittivity is calculated in accordance with temperature dependence of plasma frequency of silver nanoparticle. The effect of temperature on these structures by incorporating the volume expansion coefficient of nanoparticle is analysed. The behaviors of photonic band gaps with variation of filling factor, radii of nanoparticle and temperature are observed. The evolution of these results leads to designing the desired photonic crystals.

1. INTRODUCTION

Photonic crystals (PCs) have attracted a lot of attention in the field of optics since 1987. The most important feature of PCs is the photonic band gap (PBG), in which the existence of light is forbidden within a certain range of optical wavelengths [1]. The reason for interest in PBG materials arises from the possible applications in optical sensors, optical filters and various optical integrated devices [2, 3]. To achieve suitable band gaps, great efforts have been made to obtain tunability of the band gaps. To obtain a tunable PCs, the dielectric constant of the constituent materials must depend on some external parameters, such as electric field [4], temperature and hydrostatic pressure [5], which can modify the response functions of the PC materials.

The novel applications such as photonics, plasmonics and photovoltaics have potential in metallo-dielectric materials with plasmonics at optical and infrared wavelengths. The light sources and plasmonic metamaterials are under investigation. The use of plasmons in solar cells, cancer treatment, sensing and Plasmon based lasers has already evolved [6]. In metallic nanoparticles, the possibility of tuning their optical properties by manipulation of size, shape and the appropriate choice of host matrix has been explored to a certain extent. The size controlled optical properties of silver nanoparticles have potential applications such as diffraction elements, optical filters, nanoplasmonic devices, biosensors and nonlinear media [7].

The linear and nonlinear optical properties of composite materials are determined by plasmon resonance of metal nanoparticles and dielectric matrix. The linear and nonlinear optical properties of composite materials are determined by plasmon resonance of metal nanoparticles in transparent matrix. It is shown that optical resonance takes place in the transparent matrix with metal nanoparticles [8, 9]. The temperature dependence of the Surface Plasmon Resonance is important in most of the recent applications of noble metal nanoparticles such as thermally assisted magnetic recording [10] and computer chips [11]. In this paper, we analyze the PBG by embedding silver nanoparticles in the silica matrix. The position and width of PBG depend on the temperature dependence of dielectric permittivity of the host matrix, filling factor and for different radii of the nanoparticles. The latter is

Received 10 December 2014, Accepted 15 February 2015, Scheduled 26 February 2015

* Corresponding author: Kuladaisamy Sebastiammal Joseph Wilson (wilsonpra@yahoo.co.in).

[1] Department of Physics, K.L.N. College of Engineering, Pottapalayam 630 611, India. [2] Department of Physics, Arul Anandar College (Autonomous), Karumathur, Madurai 625 514, India.

considered through the thermal volume expansion of the nanoparticle and electron-phonon scattering in the nanoparticle.

2. THEORY

2.1. Dielectric Permittivity of Composite Material

The nanocomposite metal nanoparticles are randomly distributed in a transparent matrix. To determine the permittivity of the nanocomposite $\varepsilon_{\text{mix}}(\omega)$, we use the Maxwell-Garnett formula [12]

$$\frac{\varepsilon_{\text{mix}}(\omega) - \varepsilon_d}{\varepsilon_{\text{mix}}(\omega) + 2\varepsilon_d} = f\frac{\varepsilon_m(\omega) - \varepsilon_d}{\varepsilon_m(\omega) + 2\varepsilon_d} \tag{1}$$

where ε_d is the dielectric permittivity of the transparent matrix, f the filling factor of the nanoparticle, ε_m the dielectric permittivity of nanoparticle material, and ω the optical frequency.

When $f = 1$ (the whole volume of the matrix is occupied by metal nanoparticles), $\varepsilon_{\text{mix}} = \varepsilon_m$, and when $f = 0$ (there are no metal nanoparticle in the volume of the matrix) $\varepsilon_{\text{mix}} = \varepsilon_d$. The dielectric constant of the metal nanoparticles is determined in accordance with the drude model

$$\varepsilon_m(\omega) = \varepsilon_0 - \frac{\omega_P^2}{\omega(\omega + i\gamma)} \tag{2}$$

where ε_0 is a constant ($\varepsilon_0 = 5$ for silver [13]), ω_{p} a plasma frequency ($\omega_p = 13.64 \times 10^{15}\,\text{s}^{-1}$ [14]), and γ a damping constant of plasma oscillations. Substituting Equation (2) in Equation (1), we can deduce the real and imaginary parts of the composite material.

$$\varepsilon_{\text{mix}}(\omega) = \varepsilon'_{\text{mix}}(\omega) + \varepsilon''_{\text{mix}}(\omega) \tag{3}$$

The real and imaginary parts of $\varepsilon_{\text{mix}}(\omega)$ characterize the refractive and absorptive properties of the material. Around the resonant frequency ω', $\varepsilon'_{\text{mix}}(\omega)$ behaves in an anomalous manner, and the material exhibits strong absorption. The term $\varepsilon'_{\text{mix}}(\omega)$ is negative in particular frequency range to be denoted as ω_{10} and ω_{20}. In this interval the nanocomposite has metallic optical properties.

Nanoparticles are distributed randomly and homogenously in transparent matrix. Let us consider that silver nanoparticles are in spherical form. The plasma frequency

$$\omega_p = \sqrt{\frac{Ne^2}{m^*\varepsilon_0}} \tag{4}$$

where N is the concentration of free electron ($N = 5.85 \times 10^{28}/m^3$), e the charge of an electron, and m^* an effective mass of an free electron.

The plasmon damping constant can be expressed as [15]

$$\gamma = \gamma_\infty + A\frac{v_F}{R} \tag{5}$$

where R is the radius of the nanoparticle, γ_∞ the size independent damping constant caused by scattering of free electrons on electrons, phonons and lattice defects, $A = 1$ [15], and v_F the Fermi velocity in bulk metal ($v_F = 1.39 \times 10^6$ m/sec in bulk silver [14]). The dependence term $1/R$ in Equation (5) reflects the ratio of surface scattering probability proportional to the surface area $\mathbf{4\pi R^2}$ and the number of electrons being proportional to the volume $\frac{4\pi R^3}{3}$. This equation can be considered as a quantum size effect and reflects the surface to volume ratio [16].

The size independent damping constant γ_∞ depends on temperature due to the temperature dependence of electron-phonon scattering rate [15]

$$\gamma_\infty(T) = K'T^5 \int_0^{\frac{\theta}{T}} \frac{z^4 dz}{e^z - 1} \tag{6}$$

where $\theta = 225\,\mathrm{K}$ [17] is the Debye temperature for silver, and K' is a constant [15]. Knowing the damping constant for bulk silver at room temperature $T' = 293\,\mathrm{K}$, K' can be calculated as

$$K' = \frac{\gamma_\infty(T')}{T'^5 \int_0^{\frac{\theta}{T'}} \frac{z^4 dz}{e^z - 1}} \tag{7}$$

With the increase of temperature, the electron-phonon scattering rate increases will lead to increase of damping constant γ_∞. Due to this the permittivity of the transparent matrix is increased.

Due to thermal expansion, the radius of the nanoparticle increases as

$$R(T) = R'(1 + \beta\Delta T)^{1/3} \tag{8}$$

where R' is the nanoparticle radius at room temperature.

Because the increase of temperature makes thermal expansion of the nanoparticle, the volume of the nanoparticle increases [15]

$$V(T) = V'(1 + \beta\Delta T) \tag{9}$$

where $\Delta T = T - T'$ is the change of temperature from the room temperature and β the volume expansion coefficient for silver.

The volume expansion coefficient depends on temperature according to [15] as

$$\beta(T) = \frac{192 \in K_b}{r'\alpha(16 \in -7TK_b)^2} \tag{10}$$

where K_b is the Boltzmann constant, and $\propto, \in r'$ are the parameters of Morse potential used to describe the potential of interatomic interaction in silver

$$\mathbf{u}(\mathbf{r}) = \in \left[\mathbf{e}^{-2\alpha}(\mathbf{r} - \mathbf{r}_0) - 2\mathbf{e}^{-\alpha(r - r_0)}\right] \tag{11}$$

where $\in$ is the magnitude of the minimum well depth; α controls the shape of the potential energy curve; r is the inter atomic distance; r' is the equilibrium inter atomic distance. The parameters of Morse potential $\in = 0.3257\,\mathrm{eV}$, $\alpha = 13.535\,\mathrm{nm}^{-1}$ and $r' = 0.313300\,\mathrm{nm}$ [15].

The free electron density in a metal particle is given by $N = n/V$, where n is the number of electrons and V the particle volume. Let us consider the free electron density at room temperature be N', then the total number of free electrons in the nanoparticle is

$$n = N'V' = N(T)V(T) \tag{12}$$

The thermal expansion of the nanoparticle will lead to a decrease of concentrations of free electrons in the nanoparticle. By combining Equations (4) and (9), we can obtain the expression for temperature dependent plasmon frequency as

$$\omega_p(T) = \frac{\omega_{po}}{\sqrt{1 + \beta(T)\Delta T}} \tag{13}$$

where $\omega_{p0} = 8.9854\,\mathrm{eV}$ at room temperature.

Due to the temperature dependence of volume expansion coefficient, the plasma frequency is decreased with the increase of temperature.

2.2. Transmission Properties of Photonic Crystals

The transmission properties of one-dimensional PC consisting of nanocomposite metal nanoparticles are randomly distributed in a transparent matrix. Let us consider a one-dimensional PC, with N elementary cells with lattice constant a. Each cell consists of one nanocomposite layer of width d_1 with permittivity $\varepsilon_{\mathrm{mix}}$ and one layer of air of width d_2 with permittivity equal to 1. The lattice constant $a = d_1 + d_2$. We consider only normal incidence of electromagnetic wave on photonic crystal. We consider the value of lattice constant $a = 2\lambda_p$ where λ_p is the plasma wavelength corresponding to the plasma frequency $\omega_p(\lambda_p \equiv \frac{2\pi c}{\omega_p})$ at room temperature in Equation (13) ($\lambda_p = 138\,\mathrm{nm}$). The widths of the layers are $d_1 = 0.5a$ and $d_2 = a - d_1$.

To calculate the thickness of composite layer d_1 due to thermal expansion, we assume that the silica layer is of spherical shape of radius r ($r = \frac{d_1}{2}$) embedded with silver nanoparticle of radius R. The volume of the composite layer can be calculated as

$$V_{\text{comp}} = V_1(1 + \beta_1 \Delta T)(1 - f) + V_2(1 + \beta_2 \Delta T)f \tag{14}$$

where $V_1 = \frac{4\pi r^3}{3} - \frac{4\pi R^3}{3}$ is the volume of the silica layer, $V_2 = \frac{4\pi R^3}{3}$ the volume of the silver nanoparticle, β_1 the volume expansion coefficient of silica (1.65×10^{-6}/K [14]), β_2 the volume expansion coefficient of silver nanoparticle and f is the filling factor. The volume expansion coefficient of silver is calculated according to Equation (10) for each temperature. After expansion, the thickness of the composite layer is reassigned as $d_1 = \sqrt[3]{V_{\text{comp}}}$ for the case of one dimension. The thickness of the composite layer is reduced when the value of the filling factor is increased.

To compute the PBG in the transmission spectra due to the temperature dependence of plasma frequency, we employ the transfer matrix method **(TMM)** [18]. Each layer of PC has its own transfer matrix, and the overall transfer matrix of the system is the product of the individual transfer matrices.

For TE wave [19], each single layer has a transfer matrix according to TMM and is given by

$$M_l = \begin{pmatrix} \cos\delta_l & \frac{-i}{n_l}\sin\delta_l \\ -\text{in}_l \sin\delta_l & \cos\delta_l \end{pmatrix} \tag{15}$$

where l represents either H or L layer. The suffix H represents the nanocomposite layer, and L is the air layer.

The phase δ_1 is expressed as

$$\delta_l = k_l d_l = \frac{2\pi d_l}{\lambda} n_l \tag{16}$$

For the entire structure of Air/$(\text{HL})^N$/Air, the total transfer matrix is given by

$$T = (M_H M_L)^N \tag{17}$$

where the matrix elements can be obtained in terms of the elements of the single-period matrix. The value of N is taken as 20.

The transmission coefficient for tunneling through such a structure is given by

$$t = \frac{4}{(T_{11} + T_{22})^2 + (T_{12} + T_{21})^2} \tag{18}$$

where T_{ij} are the elements of the matrix T.

Due to thermal expansion, the thickness of air layer can be written as

$$d(T) = d(1 + \alpha \Delta T) \tag{19}$$

where α is the thermal expansion coefficient, and ΔT indicates the variation of the temperature. The thermal expansion coefficient is taken to be equal to 1/3 of volume expansion coefficient. The volume expansion coefficient of air is 3.67×10^{-3}/K [20].

The refractive index of nanocomposite layer is taken as $n = \sqrt{\varepsilon_{\text{mix}}}$ in Equation (3) and air layer as 1.

3. RESULTS AND DISCUSSION

The variation of damping constant and volume expansion coefficient with temperature are studied. The damping constant is found to increase with temperature irrespective of the size of the nanoparticle as shown in Figure 1(a). Similarly the volume expansion coefficient increases with temperature as shown in Figure 1(b).

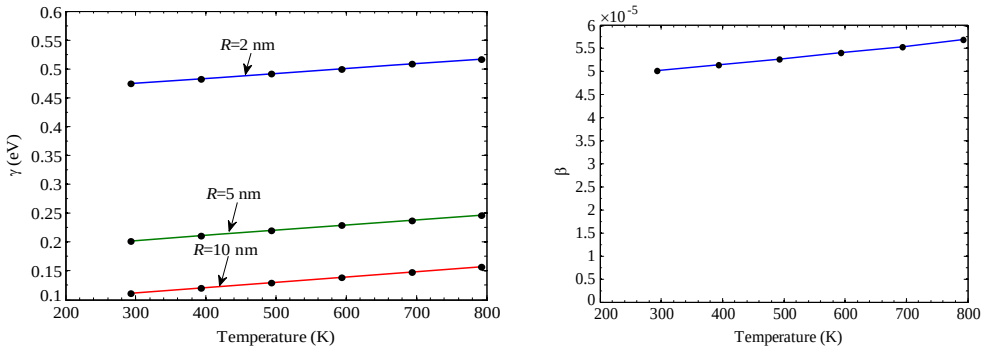

Figure 1. (a) Variation of damping constant γ and (b) volume expansion coefficient of nanoparticle β with temperature.

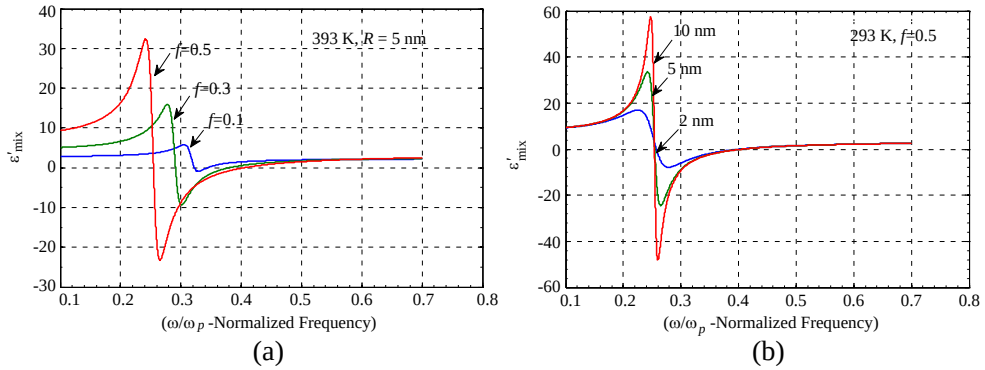

Figure 2. Real part of composite dielectric permittivity with normalized frequency (a) at 393 K for various filling factors, (b) at 293 K for various core sizes

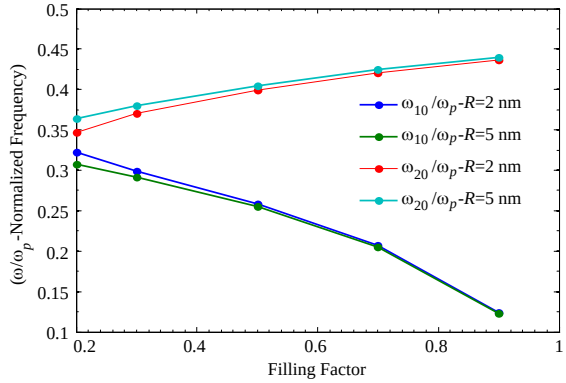

Figure 3. Dependence of ω_{10}/ω_p and ω_{20}/ω_p on filling factor at temperature 793 K.

3.1. Modulation of Dielectric Permittivity with Frequency

The filling factor strongly affects the real and imaginary parts of the dielectric permittivity of nanocomposite materials. Figure 2(a) explains the variation of dielectric permittivity with the normalized frequency for various filling factors at temperature 393 K. It is seen that the real part of the dielectric permittivity depends on the filling factor. Resonance occurs at different frequencies. The real part of the dielectric permittivity is found to be a constant and is a small value when the frequency approaches the plasma frequencies. The dielectric constant increases with the filling factor

in the low frequency region. The variation of dielectric permittivity also depends on the size of the nanoparticles. There is no appreciable variation of dielectric constant with the size of the nanoparticles except at the resonance region. At the resonance region, deviation occurs as shown in Figure 2(a). This is due to the interaction of electromagnetic radiation with plasmonic oscillations of metal nanoparticles. Plasmon resonance frequency also depends on the radius of the nanoparticles. As the filling factor changes, resonance occurs at different places as shown in Figures 2(a) and 2(b). Figure 2(b) explains the small variation in the resonance frequency, when the radius of the nanoparticles changes.

The values of ω_{10} and ω_{20} are calculated for various filling factors and radii 2 nm and 5 nm at temperature 793 K and plotted in Figure 3. When the filling factor increases, the gap between ω_{10} and ω_{20} also increases. When the size of the nanoparticles increases, deviation occurs at the lower value of the filling factor. With the increase of temperature, the gap between ω_{10} and ω_{20} also decreases. The zero value of the real part of dielectric function occurs at the two frequencies determined by the parameters of filling factor, radius of the nanoparticle and temperature. On an interval of frequencies $[\omega_{10}, \omega_{20}]$ the real part of dielectric function $\varepsilon_{\text{mix}}(\omega)$ accepts negative values of nanocomposite material similar to a metal. The width of this interval $\omega_{20} - \omega_{10}$ can be altered by changing the parameters.

The values of ω_{10}/ω_p for filling factor $f = 0.2$ are 0.3228 at radius 2 nm and 0.3075 at radius 5 nm, respectively. Similarly, the values of ω_{20}/ω_p are 0.3467 and 0.3641 for radius 2 nm and 5 nm, respectively. The dependence of frequency on filling factor for different radii at temperature 393 K is as shown in Table 1. By increasing the filling factor the value ω_{10} is shifted from visible to infrared region, and the value ω_{20} is situated in the visible region.

Table 1. Dependence of frequency on filling factor at temperature 393 K.

Radius	Filling Factor	ω_{10}/ω_p	ω_{20}/ω_p
2 nm	0.2	0.3186	0.3513
	0.3	0.2973	0.3728
	0.5	0.2577	0.4005
	0.7	0.2066	0.4210
	0.9	0.1241	0.4371
5 nm	0.2	0.3066	0.3651
	0.3	0.2910	0.3807
	0.5	0.2545	0.4054
	0.7	0.2048	0.4246
	0.9	0.1233	0.4403
10 nm	0.2	0.3051	0.3667
	0.3	0.2902	0.3819
	0.5	0.2541	0.4062
	0.7	0.2045	0.4252
	0.9	0.1231	0.4405

Table 2. Dielectric permittivity with temperature for different radii when $\omega/\omega_p = 0.2$.

Filling Factor	Radius	Dielectric Permittivity					
		293 K	393 K	493 K	593 K	693 K	793 K
0.2	2 nm	4.4756	4.4725	4.4693	4.4660	4.4627	4.4592
	5 nm	4.5392	4.5378	4.5363	4.5348	4.5332	4.5315
	10 nm	4.5494	4.5486	4.5477	4.5468	4.5458	4.5447
0.7	2 nm	12.367	12.042	11.729	11.430	11.144	10.874
	5 nm	45.456	42.307	39.422	36.818	34.472	32.322
	10 nm	108.14	97.401	87.933	79.542	72.180	65.707

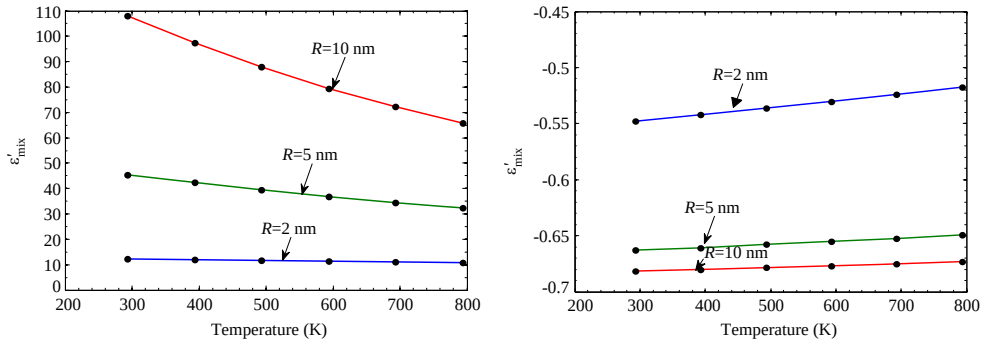

Figure 4. Real part of the composite dielectric permittivity with temperature for different radii at $f = 0.7$ for (a) $\omega/\omega_p = 0.2$, (b) $\omega/\omega_p = 0.4$.

Table 3. Position of PBG at different temperatures for parameters $f = 0.5$, $a = 2\lambda_p$, $d_1/a = 0.5$, Radius = 10 nm.

Temp.	PBG1 (ω/ω_p) eV	Width (nm)	PBG2 (ω/ω_p) eV	PBG3(ω/ω_p) eV
293 K	0.1131–0.4286	898	0.7090–0.7694	1.148–1.218
393 K	0.1084–0.4272	952.3	0.6780–0.7326	1.008–1.160
493 K	0.1037–0.4266	1012.4	0.6487–0.6911	1.034–1.093
593 K	0.1000–0.4261	1064.5	0.6276–0.6563	0.8057–0.8448
693 K	0.0961–0.4253	1123.6	0.7628–0.8099	1.120–1.181
793 K	0.0931–0.4233	1172.4	0.7312–0.7803	1.074–1.133

Table 4. Variation of refractive index with width of PBG at different temperatures for parameters $f = 0.5$, $a = 2\lambda_p$, $d_1/a = 0.5$, Radius = 10 nm.

Temp.	Width of PBG (nm)	Refractive index at (ω/ω_p)			
		0.15	0.25	0.35	0.45
293 K	898	3.3388–0.05197i	8.4847-4.4934i	0.1360–1.5505i	0.9942–0.05097i
393 K	952.3	3.3385–0.0564i	8.1640–4.5004i	0.1475–1.5497i	0.9449-0.0552i
493 K	1012.4	3.3381–0.0608i	7.8670–4.4912i	0.1590–1.5489i	0.9455–0.0595i
593 K	1064.5	3.3377–0.0653i	7.5902–4.4694i	0.1707–1.548i	0.9462–0.0639i
693 K	1123.6	3.3373–0.0698i	7.3346–4.4381i	0.1825–1.5471i	0.9470-0.0682i
793 K	1172.4	3.3368–0.0322i	7.0982–4.3997i	0.1943–1.5461i	0.9478–0.0726i

3.2. Modulation of Dielectric Permittivity of Nanocomposite with Temperature

The variation in real part of the dielectric permittivity $\varepsilon'_{\text{mix}}$ depends on the frequency. The variation in dielectric permittivity for filling factor $f = 0.7$ at radii 2 nm, 5 nm and 10 nm when $\omega/\omega_p = 0.2$ and $\omega/\omega_p = 0.4$ are shown in Figures 4(a) and 4(b). The values of the dielectric permittivity are 12.367, 45.456 and 108.14 for radii 2 nm, 5 nm and 10 nm at temperature 293 K. It is concluded that the dielectric permittivity decreases with temperatures for different radii when $\omega/\omega_p = 0.2$, but it increases when $\omega/\omega_p = 0.4$. The values of the dielectric permittivity of a nanocomposite system are calculated at various temperatures for different radii 2 nm, 5 nm and 10 nm and filling factors $f = 0.2$ and $f = 0.7$ when $\omega/\omega_p = 0.2$, which are shown in Table 2. It is shown that the value of dielectric permittivity increases with filling factor and size of the nanoparticle, but it decreases with temperature.

Table 5. Width of PBG at temperature 293 K for different radii for parameters $a = 2\lambda_p$, $d_1/a = 0.5$.

Radius	Width of PBG (nm)			
	Filling Factor			
	0.1	0.4	0.7	0.9
2 nm	444.1	854.8	1516.4	3147.2
5 nm	417.7	783.7	1317.3	2485.4
10 nm	405.1	762.3	1274	2300.9

Table 6. Position of PBG at temperature 493 K for the parameters $f = 0.3$, $a = 2\lambda_p$, $d_1/a = 0.5$.

Radius	PBG1 (ω/ω_p) eV	PBG2 (ω/ω_p) eV	PBG3 (ω/ω_p) eV	PBG4 (ω/ω_p) eV	PBG5 (ω/ω_p) eV
2 nm	0.1263–0.4855	0.6230–0.6797	1.014–1.070	1.418–1.476	1.826–1.883
5 nm	0.1282–0.4273	0.6256–0.6685	1.014–1.070	1.418–1.476	1.816–1.883
10 nm	0.1286–0.4059	0.6261–0.6686	1.015–1.070	1.419–1.476	1.827–1.884

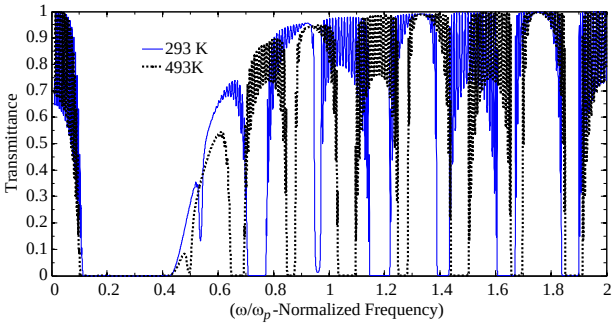

Figure 5. Transmission spectra of PBG for filling factor $f = 0.5$ at temperature 293 K and 493 K for parameters $R = 10$ nm.

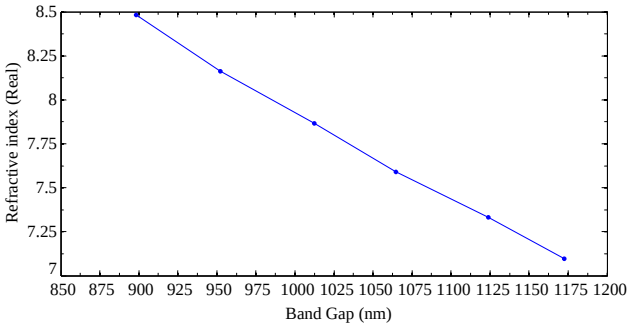

Figure 6. Variation of refractive index with PBG at different temperatures for parameters $f = 0.5$, $R = 10$.

3.3. Modulation Effects of PBG

3.3.1. Due to Temperature

On increasing the temperature, the bandgap shifts towards higher wavelength region, and the width of the PBG is increased. The transmission spectra of PBG for the size of radius 10 nm at different temperatures 293 K and 493 K for filling factor $f = 0.5$ are shown in Figure 5. We get one larger band gap in Vis-IR and many smaller band gaps in the UV region. The band gaps are specified in terms of (ω/ω_p) normalized frequency, and the frequency are calculated as $(0.1131)\ \omega_p$. The position of the PBG for filling factor $f = 0.5$ and the radius of the nanoparticle is 10 nm at different temperatures as shown in Table 3. The width of the first PBG is represented in units of wavelength. We specify some of the band gaps in the table and notice that the width of the band gaps increase while increasing the temperature. The band gaps are positioned within the range $(0.0900)\ \omega_p - (0.4500)\omega_p$.

The variation of refractive index at different values of (ω/ω_p) and the width of the PBG for different temperatures are shown in Table 4. The value of refractive index decreases when $(\omega/\omega_p) = 0.15$ and $(\omega/\omega_p) = 0.25$ and increases when $(\omega/\omega_p) = 0.35$ and $(\omega/\omega_p) = 0.45$. It is concluded that the value of refractive index depends on frequency and is high when $(\omega/\omega_p) = 0.25$. The variation in refractive index with the width of PBG when $(\omega/\omega_p) = 0.25$ is shown in Figure 6.

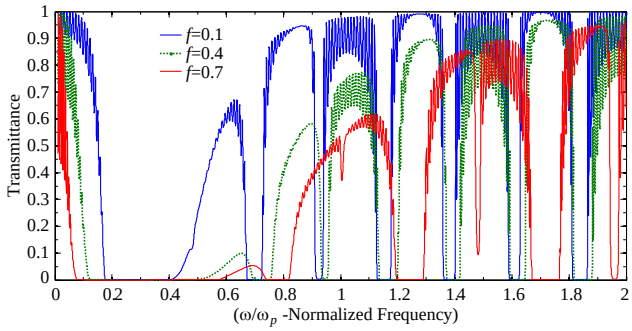

Figure 7. Transmission spectra of PBG for filling factor $f = 0.1$, $f = 0.4$ and $f = 0.7$ at temperature 293 K for parameters $R = 2$ nm, $a = 2\lambda_p$, $d_1/a = 0.5$.

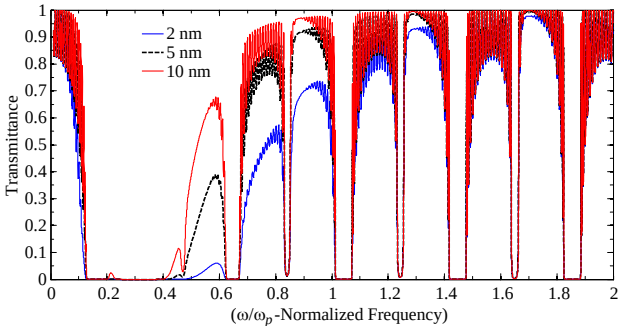

Figure 8. Transmission spectra of PBG for filling factor $f = 0.3$ at temperature 493 K for different radii when $a = 2\lambda_p$, $d_1/a = 0.5$.

3.3.2. Due to Filling Factor

Modulation effects of PBG due to filling factor for radius $R = 2$ nm at temperature 293 K is studied using Equation (7). We observe many smaller band gaps in addition to a largest band gap as shown in Figure 7. The widths of the band gap for the filling factors $f = 0.1$, 0.4 & 0.7 are shown in Table 5, which shows that the PBG increases with filling factor.

3.3.3. Due to Radius

The PBG is also analysed for different radii, i.e., $R = 2$ nm, 5 nm & 10 nm at 493 K temperature for the filling factor $f = 0.3$. The transmission spectra of the PBG for filling factor $f = 0.3$ at temperature 493 K is shown in Figure 8. By increasing the size of the nanoparticles it is found that the width of the photonic band gap decreases, and the gap shifts towards higher wavelength region. The position of PBG at temperature 493 K for $f = 0.3$ for various radii is tabulated in Table 6.

4. CONCLUSIONS

We have studied various possibilities to modify and tune the optical properties of SiO_2 matrix doped with silver nanoparticles. The value of the dielectric permittivity can be altered by changing the parameters such as the filling factor, size of the nanoparticle and temperature changes. The variation of composite dielectric permittivity with normalized frequency is analysed. It is concluded that the resonance occuring here is mainly based on the filling factor. As the filling factor changes, resonance occurs at different places. It is found that the width of the frequency range which represents the metallic optical properties is increased when the filling factor and the size of the nanoparticle increase. It is also observed that this value decreases with increase in temperature. The PBG can also be tuned by varying the size of the nanoparticles & filling factor. We conclude that we can tune the width of the photonic band gaps by changing the filling factor, size of the nanoparticle and temperature. These new optical properties can be used in manufacturing optical devices.

The TMM method employed for calculating the band gap has been used by several investigators in the past, e.g., in [19]. Also instead of SiO_2, TiO_2 has been used by Labbani and Benghalia [21]. The results obtained are in broad agreement.

Even though the band gap does not change appreciably with temperature, other physical parameters such as dielectric permittivity, volume expansion coefficient show appreciable variations which in turn provide additional information.

ACKNOWLEDGMENT

Dr. K. S. Joseph Wilson and V. Revathy acknowledge the University Grants Commission, India (Ref: No. F. 41-977/2012(SR)) for the Financial Support of this work. All authors sincerely thank Dr. K. Navaneethakrishnan, Head & Co-ordinator (Rtd.), School of Physics, Madurai Kamaraj University for his support and Guidance.

REFERENCES

1. Yablonovitch, E., "Inhibited spontaneous emission in solid-state physics and electronics," *Phys. Rev. Lett.*, Vol. 58, 3059–3062, 1987.
2. John, S., "Strong localization of photons in certain disordered dielectric superlattices," *Phys. Rev. Lett.*, Vol. 58, 2486–2489, 1987.
3. Zhang, Y., J. Wang, Y. Huang, et al., "Fabrication of functional colloidal photonic crystals based on well-designed latex particles," *J. Mater. Chem.*, Vol. 21, 14113, 2011.
4. Busch, K. and S. John, "Liquid-crystal photonic-band-gap materials: The electromagnetic vacuum," *Phys. Rev. Lett.*, Vol. 83, 967, 1999.
5. Porras-Montenegro, N. and C. A. Duque, "Temperature and hydrostatic pressure effects on the photonic band structure of a 2D honeycomb lattice," *Physica E*, Vol. 42, 1865–1869, 2010.
6. Gajc, M., H. B. Surma, et al., "Nanoparticle direct doping: Novel method for manufacturing three-dimensional plasmonic nanocomposites," *Advanced Functional Materials*, Vol. 23, 3443–3451, 2013.
7. Perez, D. P., *Silver Nanoparticles,* In-Tech Publications, 2010.
8. Oraevski, A. N. and I. E. Protsenko, "High refractive index and other properties of Heterogenic media," *JETP Lett.*, Vol. 72, 445–449, 2000.
9. Oraevski, A. N. and I. E. Protsenko, "Optical properties of heterogenous media," *Quantum Electron*, Vol. 31, 252–256, 2001.
10. Challener, W. A., C. Peng, A. V. Itagi, et al., "Heat-assisted magnetic recording by a near-field transducer with efficient optical energy transfer," *Nature Photon.*, Vol. 3, 303, 2000.
11. Cai, W., J. S. White, and N. L. Brongersma, "Compact, high-speed and power-efficient electrooptic plasmonic modulators," *Nano. Lett.*, Vol. 9, 4403, 2009.
12. Dyachenko, P. N. and Y. V. Miklyaev, "One-dimensional photonic crystal based on nanocomposite of metal nanoparticles and dielectric," *Optical Memory and Neural Networks*, Vol. 16, 198–203, 2007.
13. Johnson, P. B. and R. N. Christy, "Optical constants of the noble metals," *Phys. Rev. B*, Vol. 6, 4370–4370, 1972.
14. Tanner, D. B., "Optical effects in solids," Department of Physics, University of Florida, USA, 2013.
15. Yeshchenko, O. A. and I. S. Bondarchuk, et al., "Temperature dependence of the surface plasmon in silver nanoparticles," *Functional Materials*, Vol. 20, 357–365, 2013.
16. Quinten, M., *Optical Properties of Nanoparticle,* 2011.
17. Kittel, C., *Solid State Physics,* 8th Edition, 2011.
18. Born, M. and E. Wolf, *Principles of Optics,* 6th Edition, Peragamon, Oxford, 1980.
19. Suthar, B., V. Kumar, A. Kumar, K. S. Singh, and A. Bhargava, "Thermal expansion of photonic band gap for one dimensional photonic crystal," *Progress In Electromagnetic Research*, Vol. 32, 81–90, 2012.
20. www.engineeringtoolbox.com.
21. Labbani, A. and A. Benghalia, "Modeling by FDTD of some optical properties of photonic crystals based on a nanocomposite of silver in TiO_2," *PIERS Proceedings*, 495–498, Marrakesh, Morocco, Mar. 20–23, 2011.